Theoretical predictions of aromatic Be-O rings

Jason L. Dutton and David J. D. Wilson**

Department of Chemistry and Physics, La Trobe Institute for Molecular Science, La Trobe University, Melbourne, Victoria, Australia, 3086

ABSTRACT

We have carried out a theoretical investigation of benzene substituted with BeO to assess stability and aromatic properties (with 1-3 BeO units in a six-membered ring); C_4H_4BeO, $C_2H_2Be_2O_2$, and Be_3O_3 . All species retain a planar geometry. We considered both bare complexes and Be coordinated with L = CO, pyridine, PMe_3, and NHC. Coordination of a ligand to Be atoms causes increased Be-O bond distances. Aromatic character has been investigated with NICS and NICS-scan calculations, EDA analysis, as well as considering the energetics of hydrogenation. The complexes with the greatest aromatic character are C_4H_4BeO (**3**), and $C_4H_4Be(CO)$, which have negative $NICS(1)_{zz}$ values and minima in the NICS-scan. Coordination of two ligands to make the Be four-coordinate disrupts ring planarity and reduces aromatic character.

INTRODUCTION

Organometallic beryllium chemistry is currently undergoing a renaissance,[1, 2] however due to toxicity concerns involved in working with Be,[3] the experimental work has largely resided with a handful of groups with the special skills required to safely handle this dangerous element. However, despite the toxicity concerns, due to its small size, relatively high electronegativity and consequent tendency towards the formation of covalent bonds, Be likely has the richest and most diverse chemistry available amongst the s-block elements. Other features of Be are its small electron count and closed-shell Be(II) oxidation state in most compounds. These two properties make Be amenable to investigations using electronic-structure methods. Moreover, the toxicity concerns surrounding Be make it very attractive to conduct predictive computational investigations prior to synthetic studies. For example, our group and that of Paramesewan independently predicted the viability of N-heterocyclic carbene (NHC) stabilized Be(0) complexes,[4, 5] which were synthetically realized using the related cyclic alkylaminocarbene (cAAC) ligand in a recent ground-breaking report from the group of Braunschweig.[6] One major focus in our theoretical research program is to explore the viability of organometallic Be compounds for potential syntheses.

To date, no aromatic Be compound where Be is incorporated into the ring has been synthesized. Here we have considered six-membered rings containing Be-O for their potential stability and aromaticity. The inspiration for this work comes from borazine **1**, which has some aromatic character,[7] and may be conceived by the replacement of C-C units in benzene by isoelectronic B-N units. More recently, Liu successfully synthesized the long-sought parent single-unit B-N azaborine complex **2**,[8] which has demonstrated a rich and varied chemistry.[9, 10]

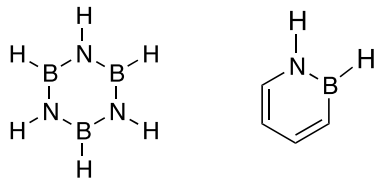

1 2

To extend this concept to Be, the Be atom must be paired with the atom one unit further to the right – O. A series of six-membered Be-O rings may be envisaged featuring one, two and three Be-O units paired with CH-CH units. Retaining the parent benzene analogue structure (with six hydrogen atoms as in **1**) would result in a cationic O-H unit and anionic Be-H unit adjacent to one another. These strongly acidic and hydridic protons next to each other would almost certainly react. However, many aromatic compounds (e.g. furan, oxazole) contain two-coordinate oxygen, so we have chosen to consider two-coordinate oxygen. Two-coordinate Be is coordinatively unsaturated and typically strongly Lewis acidic, therefore to stabilize the Be atoms in the ring, while not introducing a charge, we have chosen to evaluate compounds containing neutral ligands attached to Be. The ligands considered are CO, PMe_3, pyridine and Me_2NHC. It is expected that the two-coordinate Be would prefer to accommodate only one of these ligands to retain ring planarity, while four-coordinate Be with two ligands would generate a non-planar species.

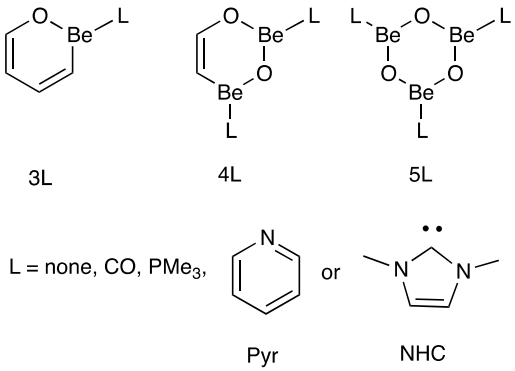

A small number of compounds with a cyclo-Be_3O_3 core have been isolated and characterized, typically with a structure of $[Be_3(\mu\text{-}A)_3(donor)_6]^{3+}$, where A is anionic O or OH.[11, 12] In each compound the cyclo-Be_3O_3 core contains three-coordinate O and four-coordinate Be atoms.

Dehnicke has reported the isolation of three compounds, namely $[Be_3(\mu\text{-}O)_3(MeCN)_6\{Be(MeCN)_3\}_3]I_2$,[13] $(Ph_4P)_2[Be_3(\mu\text{-}OH)_3(H_2O)_6]Cl_5$,[14] and $[Be_3(\mu\text{-}OH)_3(Me\text{-}Im)_6]Cl_3$.[15] It was concluded that these compounds are non-aromatic, supported by NICS calculations. Sohrin *et al*. isolated a polypyrazolylborate (scorpionate) complex of the form $[Be_3(\mu\text{-}OH)_3(HB(pz)_3)_3]$ (also labelled TpBeOH),[16] while Schulz extended that work and additionally reported the synthesis of $[Be_3(\mu\text{-}OH)_3(thf)_6]Br_3$.[17, 18] While these isolated complexes contain a cyclo-Be_3O_3 core as in **5L**, they differ to the complexes considered in this work in that we have focused on complexes with two-coordinate O atoms and three-coordinate Be atoms in the ring. Our strategy of utilising two-coordinate oxygen encourages ring planarity (and increased potential for aromaticity) and hence removes the complication of conformational flexibility (boat and chair forms) that are observed in the isolated $[Be_3(\mu\text{-}A)_3(donor)_6]^{3+}$ compounds.

Of the parent compounds **3**-**5**, only **5** has been considered previously. One paper reports B3LYP/6-311++G(2d,2p) geometries,[19] although there was no analysis of the electronic structure or properties. A separate study considering the potential of BeO clusters for hydrogen storage reported a TPSSh/6-311+G(d) calculated geometry for **5**, with a minimal analysis of electronic structure.[20] Cheng and co-workers have investigated a number of $(BeO)_n$ clusters including Be_3O_3 (**5**) also at the TPSSh/6-311+G(d) level of theory, for which geometry, HOMO-LUMO gap, and NICS calculations indicated that **5** possesses a planar geometry and aromatic character.[21] There are no previous reports of the ligand-bound **3L**-**5L** complexes.

We herein report the results of a detailed computational study of the structure, properties, and potential viability of **3L**-**5L** complexes. These novel Be compounds provide the potential of being the first Be-containing ring systems with aromatic character.

COMPUTATIONAL METHODS

Unless noted, all calculations were performed with Gaussian 09,[22] with an ultrafine DFT integration grid. Geometry optimizations were carried out with the M06-2X density functional[23] with the def2-TZVP basis set[24, 25] without any symmetry constraints. Stationary points were all characterized as minima by calculating the Hessian matrix analytically at the same level of theory. Cartesian coordinates of all optimized structures are provided in the Supporting Information. Single-point M06-2X/def2-TZVP energies were calculated at the gas-phase geometries inclusive of solvent effects using the integral equation formulation of the polarizable continuum model (IEFPCM)[26] with Truhlar's SMD solvation model[27] and acetonitrile (CH_3CN) solvent parameters. All reported ΔG values are solvent-corrected electronic energies with gas phase thermochemical corrections (standard conditions of T = 298.15 K and p = 1 atm). Natural bond orbital (NBO)[28] and molecular orbital analysis was carried out at the M06-2X/def2-TZVP level of theory including solvent effects. NICS and NICS-scan calculations were carried out at the B3LYP/6-311+G(d,p) level of theory within the GIAO approach. NICS-scan calculations employed the Aroma program.[29] EDA and EDA-NOCV calculations were performed using the ADF package.[30] BP86 was chosen for the application of uncontracted Slater-type orbitals (STOs) as basis functions.[31] The latter basis sets for all elements have double-ζ quality augmented by one set of polarization functions (ADF-basis set DZP). This level of theory is denoted BP86/DZP. An auxiliary set of s, p, d, f, and g STOs was used to fit the molecular densities and to represent the Coulomb and exchange potentials accurately in each SCF cycle.[32] Scalar relativistic effects have been incorporated by applying the zeroth-order regular approximation (ZORA) in all ADF calculations.[33]

RESULTS AND DISCUSSION

1. Geometrical Properties

Compound 3 ($BeOC_4H_4$) and 3L ($LBeOC_4H_4$)

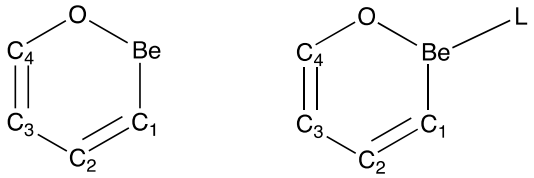

Compound **3** features a Be-O bond distance of 1.449 Å (Table 1), which is shorter than in the isolated $[Be_3(\mu\text{-}A)_3(donor)_6]^{3+}$ compounds that are in the range of 1.550-1.604 Å,[13-18] but in closer agreement with 1.470 Å in the β-diketiminate complex [^{Ph}LBeO$(CH_2)_4$I] reported by Hill.[34] The Be-O bond distance is shorter than the sum of single-bond covalent radii from the empirical fit of Pyykko (1.65 Å),[35] but greater than the calculated bond distance of 1.318 Å (WBI 0.42) for free BeO with a formal double bond, which is suggestive of partial double-bond Be-O character in **3**. The Be-C bond distance in **3** is 1.628 Å. This compares to 1.703-1.710 Å in [t-BuC$(NAr)_2$]BeEt,[36] and 1.745-1.757 Å for the single covalent Be-C_{Ph} bond in NHC-$BePh_2$.[37] Braunschweig reported Be-C distances of 1.657-1.664 Å in BeL_2 (L = cAAC), which were suggested to display partial Be-C double bond character.[6] The sum of empirical single-bond covalent radii for Be-C is 1.77 Å,[35] which is consistent with the Be-C bonds in **3** and Braunschweig's BeL_2 compounds containing partial double-bond character.

The C-C bonds are more localized than in benzene, with a calculated C_1-C_2 distance of 1.362 Å, C_2-C_3 at 1.457 Å and C_3-C_4 of 1.349 Å. Wiberg bond indices (WBI) of 1.86, 1.16 and 1.72 further emphasise the localised C-C and C=C bonding character in **3**. For comparison, in the less aromatic furan the C-C bond distances are calculated to be 1.351 and 1.433 Å, respectively. The corresponding C-C bond distances in azaborine (**2**) are calculated to be 1.357, 1.422 and 1.366 Å, respectively.

Table 1. Optimized bond distances (Å) and Wiberg Bond Indices (WBI, parentheses) for compounds **3L**, L-$BeOC_4H_4$.

Bond	Ligand (L)				
	none	CO	PMe_3	pyridine	Me_2NHC
Be-O	1.449 (0.20)	1.483 (0.19)	1.505 (0.17)	1.505 (0.17)	1.522 (0.16)
Be-C1	1.628 (0.38)	1.654 (0.33)	1.673 (0.32)	1.678 (0.33)	1.695 (0.30)
O-C4	1.344 (1.11)	1.327 (1.13)	1.328 (1.13)	1.328 (1.13)	1.324 (1.14)
C1-C2	1.362 (1.86)	1.362 (1.83)	1.359 (1.84)	1.358 (1.85)	1.358 (1.85)
C2-C3	1.457 (1.16)	1.447 (1.17)	1.450 (1.16)	1.452 (1.16)	1.449 (1.16)
C3-C4	1.349 (1.72)	1.352 (1.68)	1.350 (1.69)	1.349 (1.69)	1.350 (1.68)

The **3L** compounds display a planar geometry in all cases, as expected for formally sp^2-hydribized three-coordinate Be atoms paired with two-coordinate O atoms. That there is no deflection from planarity indicates that the compounds all fulfil the geometrical requirements to be aromatic. To analyse the bonding in **3L**, the complexes may be discussed as a single set as the effect on endocyclic bonds when varying the external ligand is only minor. In comparison with the free compound **3**, complexation serves to elongate the Be-O bond distances, which range from 1.483 (L=CO) to 1.522 (L=NHC) Å. Analogous to **4L**, the Be-O bond distances increase in the order of **3NHC** > **3pyr** > **3PMe$_3$** > **3CO** > **3**. The longer bond distances in **3L** are in closer agreement with the Be-O bonds in the isolated $[Be_3(\mu\text{-}A)_3(donor)_6]^{3+}$ compounds (1.550-1.604 Å).[13-18] The Be-C bonds range from 1.654 to 1.695 Å, which are elongated compared to 1.628 Å in free **3**. In contrast, the endocyclic C-O bond distances (1.324-1.327 Å) are slightly compressed compared to free **3** (1.344 Å). The ring C-C bonds are consistent with **3**, with the C_1-C_2 (1.358-1.362 Å) and C_3-C_4 (1.349-1.352 Å) distances almost identical to **3** (1.362 and 1.349 Å, respectively), while C_2-C_3 distances in the complexes (1.447-1.452 Å) are slightly shorter than in **3** (1.457 Å). The minimal effect of complexation on the endocyclic C-C bonds is reflected in calculated WBI values, with a maximum deviation of only 0.03 for C-C bonds between **3L** and **3**. The exocyclic bonds

between the Be atoms and the ligands are typical for single bonds between Be and C, P and N, respectively.

Compound 4 ($Be_2O_2C_2H_2$) and 4L ($L_2Be_2O_2C_2H_2$)

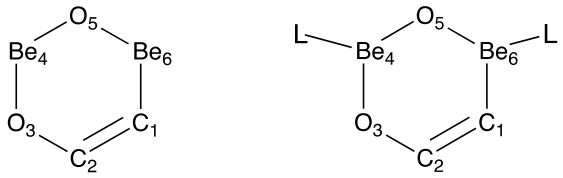

Both the parent compound **4** and ligated **4L** complexes exhibit a planar ring geometry. For all **4L** complexes, the Be-O bonds exhibit consistent trends: Be_4-O_5 and Be_6-O_5 bond distances are generally similar, while Be4-O3 is about 0.3 Å longer (Table 3). As a result, the Be_4-O_5 and Be_6-O_5 bond distances are shorter than in **3L**, while the Be_4-O_3 distance is longer than in **3L**. The Be-O bonds are shortest in the free compound **4** (1.671 Å), with **4NHC** exhibiting the longest Be-O bond distances (1.730 Å). For each L, the Be-C bond distance is marginally shorter in **4L** than in **3L**. The C_1-C_2 bond is localized and consistent at 1.346-1.349 Å (WBI 1.87-1.90) for all **4L** complexes, indicating increased double bond character relative to **3L**. Addition of the ligands increases the Be-O bond distances relative to **4**, while the ligands have virtually no effect on the endocyclic C-C bond.

Table 2. Optimized bond distances (Å) and Wiberg Bond Indices (WBI) in compounds **4L**, L_2-$Be_2O_2C_2H_2$.

Bond	Ligand (L)				
	none	CO	PMe_3	pyridine	Me_2NHC
Be_6-O_5	1.439 (0.23)	1.465 (0.21)	1.473 (0.22)	1.484 (0.22)	1.499 (0.19)
Be_4-O_5	1.434 (0.25)	1.451 (0.22)	1.470 (0.21)	1.471 (0.23)	1.482 (0.20)
Be_4-O_3	1.461 (0.21)	1.489 (0.22)	1.504 (0.18)	1.515 (0.19)	1.529 (0.17)
Be_6-C_1	1.671 (0.37)	1.692 (0.32)	1.715 (0.28)	1.717 (0.31)	1.730 (0.29)
C_2-O_3	1.367 (1.05)	1.353 (1.07)	1.347 (1.08)	1.350 (1.08)	1.346 (1.08)
C_1-C_2	1.347 (1.90)	1.349 (1.87)	1.349 (1.87)	1.346 (1.88)	1.347 (1.87)

Compound 5 (Be_3O_3) and Compound 5L ($L_3Be_3O_3$)

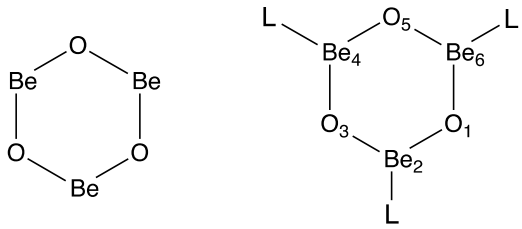

The parent compound Be_3O_3, **5**, has been considered previously.[19, 20] Our M06-2X/def2-TZVP geometry is consistent with the previously reported B3LYP/6-311++G(2d,2p) and TPSSH/6-311+G(d) calculated geometries, similarly predicting a D_{3h} symmetry structure. The M06-2X calculated Be-O bond distance of 1.453 Å (Table 4), is comparable to the B3LYP (1.450 Å)[19] and TPSSH (1.461 Å)[20] results, and similar to 1.449 Å calculated for free compound **3**. The calculated WBI value of 0.24 in **5** is marginally greater than in **3** (0.20), consistent with the bond distance trend. The **5L** complexes display a planar Be_3O_3 geometry in all cases, with Be-O bond distances elongated relative to **5**. Again, Be-O bond distances follow the trend that **5NHC** > **5pyr** > **5PMe$_3$** > **5CO** > **5**.

Table 3. Optimized bond distances (Å) and Wiberg Bond Indices (WBI) for compounds **5L**, L_3-Be_3O_3.

Bond	Ligand (L)				
	none	CO	PMe_3	pyridine	Me_2NHC
Symmetry	D_{3h}	C_{3h}	C_{3h}	C_{3h}	D_3
Be-O	1.453 (0.24)	1.471 (0.22)	1.479 (0.21) [a]	1.492 (0.21)	1.504 (0.19)

[a] Alternating Be-O distances of 1.492 Å (WBI 0.20) and 1.479 Å.

2. Ligand Binding Energetics

An important measure of the stability of the heterocyclic ring (and aromatic character) is the energetics of binding ligands. M06-2X/def2-TZVP calculated binding free energies, inclusive of solvent effects (CH_3CN solvent), are collated in Table 4. Calculated ΔG for ligand exchange reactions

provide consistent trends for **3L-5L**, with ligand binding in the order NHC > pyridine > PMe_3 > CO (Table 4). For **3L-5L**, the addition of a second ligand to each Be atom was investigated to form **3L$_2$-5L$_2$**. For **3**, the addition of ligands to Be to form **3L** is favourable for all ligands considered, with Me_2NHC being the most favourable at -126.3 kJ/mol. CO, PMe_3 and pyridine have binding free energies of 13.9, 72.1 and 108.3 kJ/mol, respectively. This indicates that the addition of neutral ligands should provide stability to these compounds. Beryllium typically prefers to be 4-coordinate, however addition of a second ligand to any of **3L** to form **3L$_2$** is generally endergonic, with the exception of pyridine, which is slightly exergonic at -8.8 kJ/mol.

The addition of a ligand to each of the Be atoms is also favourable for compounds **4** and **5**, again with NHCs having the largest negative free energy change for addition at -196.2 and -233.5 kJ/mol for **4** and **5**, respectively. For all ligands, the binding free energy per ligand is greatest in **3**, and reduces in **4** with **5** exhibiting the smallest binding free energy. With Me_2NHC, the binding free energy per ligand is -126.3 kJ/mol (**3**), -98.1 kJ/mol (**4**) and -77.8 kJ/mol (**5**). Binding of a second ligand to each Be atom in **4** and **5** is unfavourable, with ΔG becoming more endergonic from **3** to **4** and finally **5**.

Table 4. M06-2X/def2-TZVP calculated free energies (ΔG, kJ/mol) for the addition of ligands to **3-5**.

	Ligand			
	CO	PMe_3	pyridine	Me_2NHC
3 + L	-13.9	-72.1	-108.3	-126.3
4 + 2L	[a]	-88.8	-174.5	-196.2
5 + 3L	-2.5	-79.5	-221.8	-233.5
3L + L	+26.1	+14.4	-8.8	+6.8
4L + 2L	[a]	+61.8	+31.8	+78.5
5L + 3L	+53.9	+70.0	+113.2	

[a] No minima located, second CO ligand dissociates.

The consistent trend in ligand binding energies for **3-5** being in the order of Me_2NHC > pyridine > PMe_3 > CO. Interestingly, that matches the variation in Be-O bond distances upon complexation

(Me_2NHC > pyridine > PMe_3 > CO). To further explore the nature of ligand binding and its effect on the electronic structure of the ring, we have carried out energy decomposition analysis (EDA) calculations for **3L** compounds at the B3LYP/DZP level of theory. Results are presented in Table 5. Note that the interactions energies (ΔE_{int}) are not directly equated to dissociation energies (D_e) since ΔE_{int} is calculated with fragments at the geometry of the optimized complex.

Table 5. Results of EDA calculations (BP86/DZP, kJ/mol) for **3L** (L = CO, PMe3, pyridine, Me_2NHC).

	CO	PMe_3	Pyridine	Me_2NHC
ΔE_{int}	-91.0	-165.6	-194.2	-262.3
ΔE_{Pauli}	158.9	195.6	251.0	302.3
ΔE_{elstat}	-113.1 (45.3%)	-206.6 (57.2%)	-272.4 (61.2%)	-361.2 (64.0%)
ΔE_{orb}	-136.8 (54.7%)	-154.7 (42.8%)	-172.9 (38.8%)	-203.4 (36.0%)

[a] The values in parentheses are the percentage contributions to the total orbital interactions $\Delta E_{Elstat} + \Delta E_{Orbital}$.

The intrinsic interaction energy for the complexes follows the trend of ligand binding energies. Indeed, each component (ΔE_{Pauli}, ΔE_{elstat}, and $\Delta E_{orbital}$) increase in magnitude from CO to Me_2NHC. Interestingly, the covalent (orbital) contribution to the total attraction decreases from CO to Me_2NHC, which suggests that while CO exhibits the weakest ligand binding energy, it possesses the greatest covalent character. We have calculated deformation densities $\Delta\rho$, which are associated with the most important orbital interactions between the fragments. With the EDA-NOCV method it is possible to calculate pairwise contributions to $\Delta E_{orbital}$. Figure 1 shows deformation densities for **3CO** and **3NHC**. Note that the colour denotes charge flow, which is from red to blue. Visual inspection indicates that the largest pairwise contribution to the orbital interaction arises from **3←L** σ donation, while **3→L** π back-donation is observable yet smaller in magnitude. The nature of the $\Delta\rho$ associated with π back-donation is indicative of π delocalization (and out-of-plane p_z occupation) of the Be atom. For **3CO**, there is charge flow from the ring (especially the atoms neighbouring Be) to the exocyclic Be-C π-bond orbital, which suggests that the Be p_z orbital is at least partially occupied with

resultant delocalization. For **3NHC**, π back-donation mostly arises from reorganization of the NHC ring, with donation to the p_z orbital of the carbene carbon, with little evidence of any exocyclic Be-C π-bond. Similar analysis of **3PMe$_3$** and **3pyr** indicates that they are intermediate between **3CO** and **3NHC**. The trend may be related to the π accepting ability of the ligand, whereby CO and PR_3 are better π acceptors than pyridine and NHC.

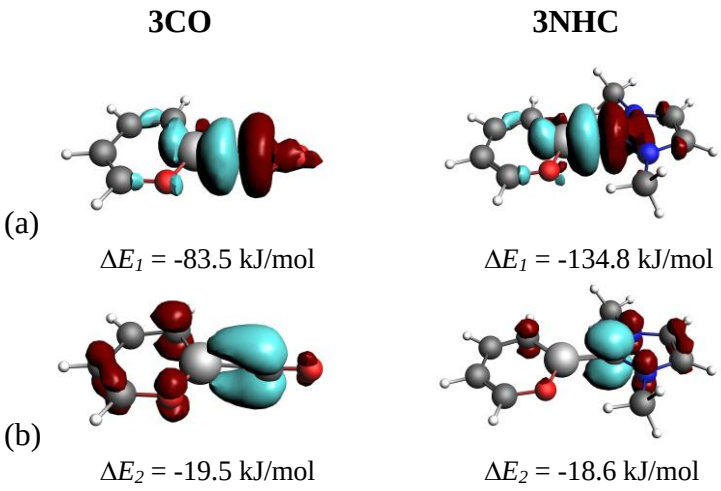

Figure 1. Deformation densities $\Delta\rho$ with the most important orbital interactions of **3CO** and **3NHC**. The direction of the charge flow is red → blue. (a) Deformation density due to **3←L** σ donation. (b) Deformation density due to **3→L** π back-donation.

The greatest variation in Be-O bond distance compared to **3** occurs in **3NHC**, which is consistent with the largest binding energy for Me_2NHC. Moreover, the EDA-NOCV analysis suggests that there is greatest π delocalization in **3CO**, which reduces to **3NHC**; the more strongly bound ligands disrupt the contribution of Be to the π system of the ring, which serves to reduce aromaticity and lengthen the Be-O bond.

3. Aromaticity

Nucleus-independent chemical shift (NICS)[38] and NICS-scan[39] calculations provide an assessment of aromatic character. For NICS(1) shielding, calculated 1 Å perpendicular to the ring, a negative value is indicative of aromatic character, while a NICS-scan that exhibits a minimum in the out-of-plane component of the shielding is indicative of aromaticity (diatropic ring current). We performed NICS and NICS-scan calculations on compounds **3L**, **3L$_2$**, **4L** and **5L**, with aromatic benzene, furan, phosphole, and azaborine, and antiaromatic cyclobutene included for comparison. B3LYP/6-311+G(d) results for NICS(1) are presented in Table 6, for both the isotropic and out-of-plane components of the shielding. Plots of NICS-scan results are given in the Supporting Information, with representative examples illustrated in Figure 2.

We have considered two components of NICS(1): the isotropic NICS(1)$_{iso}$ shielding (labeled simply as NICS(1)) and the out-of-plane component, NICS(1)$_{zz}$. The NICS(1) for benzene, the benchmark molecule for strong aromaticity, is -10.1 ppm while the NICS(1)$_{zz}$ component is -29.1 ppm. Furan yields values of -9.4 ppm (isotropic) and -27.4 ppm (out-of-plane), while phosphole gives values of -6.1 ppm and -20.1 ppm, respectively. The NICS(1) and NICS(1)$_{zz}$ for azaborine are -7.0 ppm and -20.1 ppm, which are smaller in magnitude than the previously reported B3LYP/6-311+G(d,p) results (-10.2 and -29.2 ppm, respectively).[40] The deviation can be ascribed to the different methods employed in the geometry optimization.

For the NICS-scan results (Figure 2), benzene possesses a clear minimum which is indicative of aromatic character, at a distance of about 1 Å from the ring, which coincides with the NICS(1) criteria being calculated at 1 Å from the plane of the ring. For the reference aromatic compounds considered here, the depth of the well is consistent with the magnitude of the NICS(1)$_{zz}$ value, with benzene > furan > azaborine > phosphole. For the anti-aromatic cyclo-butadiene all NICS-Scan results are positive in sign with no minimum in the NICS-Scan plot, which is indicative of anti-aromatic character.

Table 6. B3LYP/6-311+G(d) calculated isotropic NICS(1) and out-of-plane NICS(1)$_{zz}$ (parentheses) values (ppm).

	Ligand (L)				
Compound	none	CO	PMe_3	pyridine	Me_2NHC
3L	-3.2 (-8.1)	-4.1 (-11.2)	-3.2 (-8.4)	-2.3 (-5.8)	-2.8 (-7.5)
4L	-3.5 (-0.2)	-1.4 (-1.9)	-0.8 (+0.6)	0.0 (+2.8)	-0.4 (+1.8)
5L	-1.2 (+0.4)	-1.4 (+0.3)	-1.1 (+2.8)	-0.1 (+5.0)	-0.5 (+4.1)
$3L_2$		-0.8 (-0.9)	0.0 (-1.8)	+0.2 (+1.6)	[a]
benzene	-10.2 (-29.1)				
furan	-9.4 (-27.4)				
azaborine	-7.0 (-20.1)				
phosphole	-6.1 (-13.6)				
cyclobutene	+18.1 (+57.2)				

[a] Non-planar ring geometry

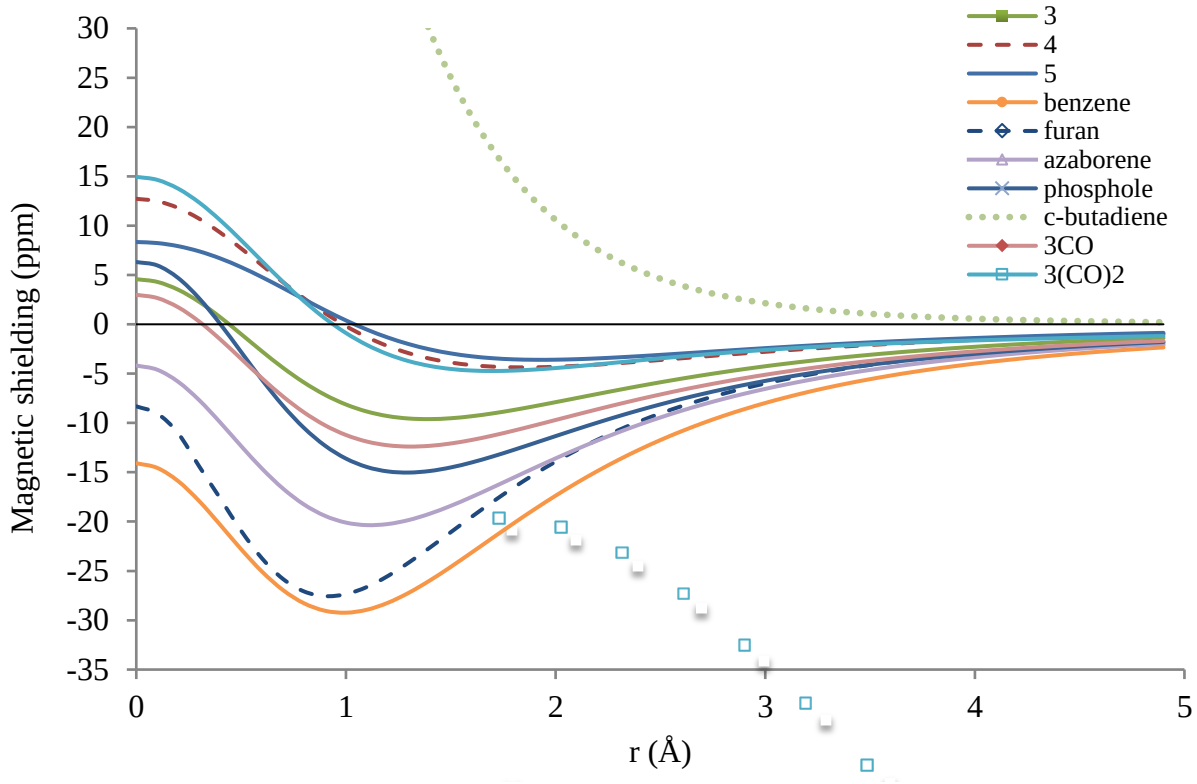

Figure 2. NICS-Scan results (out-of-plane zz component, ppm) as a function of distanceq above the ring (Å) for **3-5**, **3CO**, **3(CO)$_2$**, benzene, furan, azaborine, phosphole and cyclo-butadiene.

For the anti-aromatic compound cyclobutadiene, the NICS(1) and NICS(1)$_{zz}$) values are +18.1 ppm and +57.2 ppm, respectively, with the large positive values reflecting the anti-aromatic character. Trends are consistent between the isotropic and out-of-plane NICS(1) values, and hence for the purpose of comparison of NICS(1) and NICS-scan, subsequent discussion of NICS will be limited to the out-of-plane NICS(1)$_{zz}$ of the shielding.

Parent compound **3** exhibits a shallow well, with a minimum of -9.6 ppm at a distance 1.4 Å from the ring; the NICS(1)$_{zz}$ value at 1 Å is smaller in magnitude at -8.1 ppm. Addition of a single ligand to **3** does not significantly affect the NICS-scan trends, with minima for each **3L** and well-depths that range from 12.4 ppm (CO) to 8.3 ppm (pyridine). In comparison, **3L** gives a range of out-of-plane NICS(1)$_{zz}$ from -11.2 ppm (CO) to -5.8 (pyridine). These values show that in all cases the analogues of **3** are clearly less aromatic than species such as azaborine and benzene. However, addition of a second ligand to the beryllium atom (**3L$_2$**), which breaks the planarity of the ring and possible p-orbital conjugation of the ring, results in a loss of the minima, as illustrated for L=CO (**3(CO)$_2$**) in Figure 2, and more positive NICS(1)$_{zz}$ values of -1.8 to +1.6 ppm (Table 6).

Compounds **4L** and **5L**, with or without ligands, all exhibit minima in the NICS scan although the well depths of 2.5-4.0 ppm (**4L**) and 3.4-5.5 ppm (**5L**) are much shallower than for **3L** (8.3-12.4 ppm). Addition of a second ligand to each Be atom in **4L** and **5L** disrupts the ring planarity such that NICS-scan calculations are not possible. For compound **5**, Cheng has reported a NICS(0) value of -6.44 ppm at the TPSSh/6-311+G(d) level of theory. For comparison, the B3LYP/6-311+G(d,p) result for NICS(0) is -4.2 ppm. While the results are method dependent, in both cases the sign is negative and indicative of aromatic character in **5**.

The presence of a minima indicates the presence of aromatic character. However, the minimum in the NICS-scan occurs at a greater distance from the ring in **4L** and **5L**, and generally increases with the number of BeO units in the ring. For **3L**, minima occur at 1.3-1.5 Å from the ring, while for **4L** the minima occur at 1.2-2.2 Å from the ring, and for **5L** it is 1.9-2.7 Å.

For carbon-based systems most NICS-scan plots yield a minimum at about 1 Å out of the ring plane, however it is not necessarily the case for all heterocyclic systems. The diatropic and paratropic out-of-plane NICS effects primarily originate from the π system, whereby the presence of heteroatoms in the ring with different size p orbitals compared to carbon will produce differences in the π system. Subsequently, it can be expected that the maximum diatropic effect will occur at different distances from the ring plane. For the BeO systems, the minimum in the out-of-plane NICS-scan occurs further from the plane of the ring than for the aromatic reference systems, which is indicative of a smaller diamagnetic ring current in the BeO systems. The increasing distance of the minimum from **3** to **5** further suggests a successive reduction in diamagnetic rung current (and reduced aromaticity) from **3** to **5**.

The plots for **3** and **3L** are similar to that for phosphole, being paratropic (positive in sign) at short distances from the plane and becoming diatropic (negative in sign) at larger distances. Since the out-of-plane NICS effect is largely based on the π system, it is suggested that the BeO heteroatoms in **3L** contribute to the π system to a similar degree as P does in phosphole. For **4L**-**5L**, with NICS-Scan minima at greater distances from the plane, similar analysis suggests that the BeO units contribute less to the π system. Further support for this analysis is provided below an investigation of molecular orbitals of these systems.

4. H_2 addition reaction

Energy of hydrogenation of the ring is another indicator of possible aromaticity. As is taught to all undergraduate chemistry students, the addition of H_2 to benzene is unfavourable, while the addition of H_2 to non-aromatic cyclohexene is favourable. Hydrogenation of **3L** and **3L**$_2$ was investigated, with addition of H_2 to the CH-CH group neighboring either the Be and O atoms in the ring being considered. For compound **3**, hydrogenation at the C-C bond adjacent to Be (ΔG is -37.0 kJ/mol) is preferable to hydrogenation at the C-C bond adjacent to O (-25.3 kJ/mol). For the ligand bound

complexes **3L** and **3L$_2$**, hydrogenation is similarly predicted to occur at the C-C bond adjacent to beryllium.

Calculated results for hydrogenation of **3L** and **3L$_2$** are presented in Table 7. For reference, at the same level of theory we calculated Δ*G* for the addition of H_2 to aromatic benzene (+66.6 kJ/mol) and anti-aromatic cyclohexene (-78.9 kJ/mol), which is consistent with hydrogenation being non-favourable for aromatics and favourable for non-aromatic compounds. For furan, addition of H_2 across the C-C bond adjacent to oxygen has a Δ*G* of -6.0 kJ/mol, while for azaborine we calculate the Δ*G* of hydrogenation to be +4.0 kJ/mol for hydrogenation of the C atoms adjacent to boron. For non-aromatic (non-planar at P) phosphole we calculate Δ*G* of hydrogenation to be -55.5 kJ/mol.

Table 7. M06-2X/def2-TZVP calculated free energy of hydrogenation (Δ*G*, kJ/mol).

	Ligand (L)				
	None	CO	PMe_3	pyridine	Me_2NHC
3L + H_2	-37.0	-30.1	-21.2	-27.5	-26.1
3L$_2$ + H_2		-42.3	-30.3	-36.0	-34.8
3L(H$_2$) + H_2	-69.4	-62.9	-50.8	-55.2	-55.0
3L$_2$(H$_2$) + H_2		-56.7	-23.1	-39.7	-44.1
benzene	+66.4				
azaborine	+4.0				
furan	-6.0				
phosphole	-55.5				

The addition of H_2 is exergonic for each ligand, however smaller in magnitude compared to **3**. With two ligands bound to Be in **3L$_2$**, which breaks planarity and conjugation, the free energy for H_2 reduction becomes more favourable by about 10 kJ/mol (relative to **3L**), despite the molecule being overall more electron rich having the second donor ligand bound. Again, while less aromatic behavior than benzene, furan and azaborine is apparent, there is some evidence of aromatic character in the Be-O analogues **3L**.

For all **3L** compounds, the free energy of hydrogenation is more negative than for the reference furan and azaborine aromatic compounds, which is consistent with other aromaticity properties discussed above. However, ΔG for **3L** are more positive than for phosphole, which suggests that **3L** are more aromatic than phosphole.

The addition of a second H_2 leading to saturate the C-C bonds is exergonic for all **3L** compounds. The free energy of hydrogenation is more favourable for **3L(H$_2$)** (-51 to -69 kJ/mol) compared to **3L** (-21 to -37 kJ/mol), which is indicative of hydrogenated **3L** (i.e. **3L(H$_2$)**) being less aromatic than **3L**.

5. Molecular Orbital Analysis

The frontier molecular orbitals were calculated for all compounds. A small HOMO-LUMO gap can be an indicator of instability for small molecules.[41] It is important to note that the HOMO-LUMO gap has a strong DFT functional dependence (and specifically the proportion of Hartree-Fock exchange), for which the M06-2X functional with 54% Hartree-Fock exchange will produce larger HOMO-LUMO gaps than other functionals such as B3LYP (20%) and BP86 (0%). Nevertheless, the trends will be reliably reproduced by the different functionals.

There is a general trend in the HOMO-LUMO gaps, with **3L** < **4L** < **5L** for each ligand. Moreover, addition of a second ligand to each Be atom (**3L$_2$**, **4L$_2$**, **5L$_2$**) reduces the HOMO-LUMO gap. For **3**, the M06-2X/def2-TZVP calculated HOMO-LUMO gap is 7.49 eV, while for **3L** with a ligand bound to Be the HOMO-LUMO gaps are in the range of 6.13 to 7.24 eV (Table 8). The B3LYP/def2-TZVP results are smaller in magnitude, however in both cases the magnitude of HOMO-LUMO gaps indicate these molecules are likely to be electronically viable species in the condensed phase.

Table 8. M06-2X/def2-TZVP and B3LYP/def2-TZVP (parentheses) calculated HOMO-LUMO gaps (eV).

	Ligand (L)				
	None	CO	PMe_3	Pyridine	Me_2NHC
3L	7.49 (5.17)	6.15 (3.59)	7.24 (5.02)	6.13 (3.80)	6.96 (4.73)
4L	7.63 (5.66)	6.71 (3.89)	7.60 (5.66)	6.44 (3.94)	7.47 (5.16)
5L	9.40 (6.92)	8.65 (5.39)	8.24 (6.43)	7.80 (4.88)	8.45 (6.07)

For **4** and **4L** the M06-2X/def2-TZVP calculated HOMO-LUMO gaps are 7.63 and 6.44-7.60 eV, respectively, while for **5** and **5L**, the HOMO-LUMO gaps are 9.40 and 7.80-8.65 eV, respectively, which are also relatively large in both cases. The B3LYP/def2-TZVP results are smaller in magnitude but nevertheless are relatively large.

Plots of the frontier MOs are presented in Figure 3, including the HOMO, LUMO and other relevant π-symmetry MOs. Plots of frontier MOs for parent **3**-**5** compounds as well as **3L**-**5L** with CO and pyridine ligands are provided in the Supporting Information. In each case the HOMO is a π-symmetry orbital in the ring. For **3** with no ligand, the π delocalization is more apparent than with **4** and **5**, with involvement from both the O and C atoms. There is a minor contribution from the Be atom, which indicates the Be atom is participating in the π -system of the ring.

The LUMO in **3** is a σ-symmetric orbital centred on the Be atom, along the vector the ligand occupies in **3L**. In **3L**, the Be-L sigma MO is relatively low in energy with the LUMO being a π-symmetric orbital on the Be-L bond. In contrast, for **4** and **5** there is reduced delocalization involving the Be atom; with **5** the occupied π-symmetric orbitals have virtually all of their coefficient localized on the O atoms. The greater π delocalization in **3** is consistent with the NICS and NICS-scan analysis, in that **3** is predicted greater aromatic character than **4** or **5**. It is also consistent with the analysis from the location of the minima in the NICS-scan being indicative of the degree of contribution of the heteroatom to the π system.

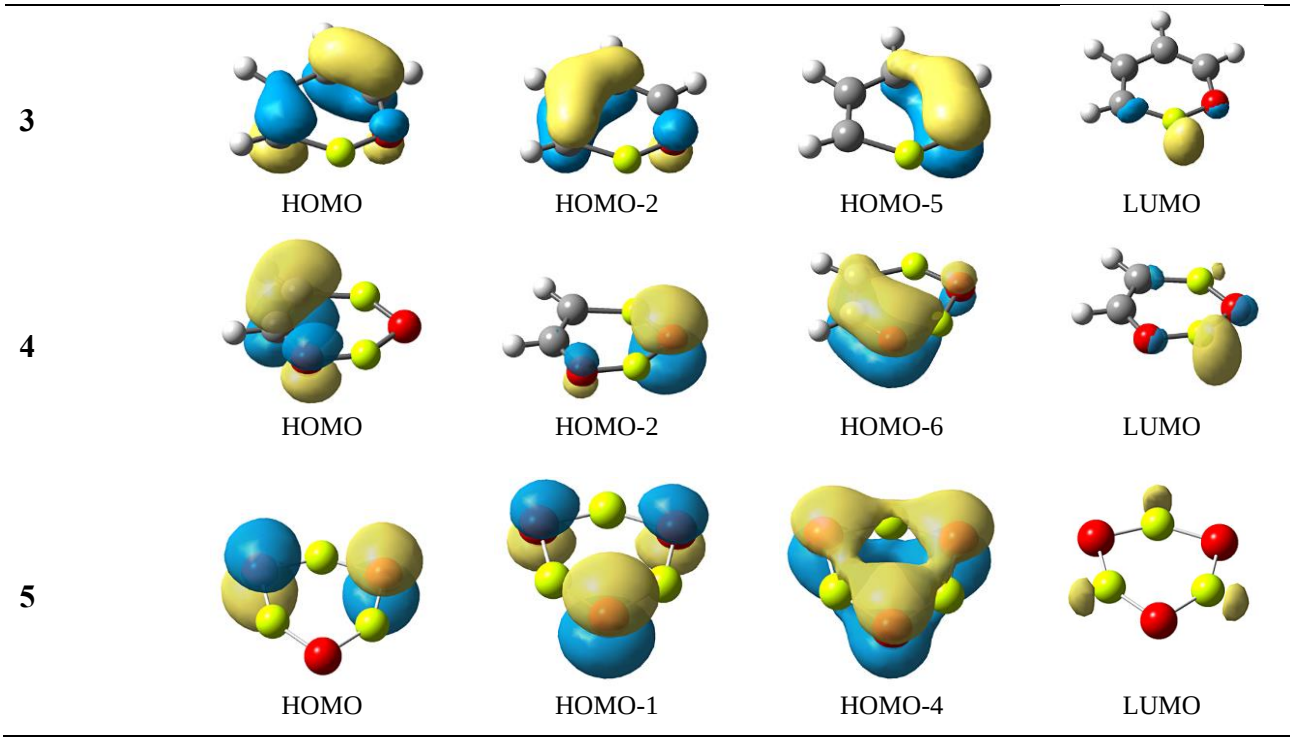

Figure 3. Plots of frontier molecular orbitals for **3**, **4** and **5**.

CONCLUSIONS

A theoretical investigation of benzene substituted with BeO (with one to three BeO units in a six-membered ring) indicates that all rings possess a planar ring geometry. In each case, complexes with Be coordinated to ligands of L = CO, pyridine, PMe_3, and NHC were also considered. Coordination of a single ligand to Be atoms does not disrupt the planar geometry but causes increased Be-O bond distances, while coordination of a second ligand to make the Be four-coordinate disrupts the ring planarity and reduces aromatic character. Aromatic character has been investigated with NICS and NICS-scan calculations, as well as considering the energetics of hydrogenation. From analysis of MOs, NICS and NICS-scan, hydrogenation reactions and ligand binding, it is concluded that the compound generated by substitution with a single BeO molecule (**3L**) has some aromatic character, likely greater than in phosphole, and as such is an interesting target for synthetic chemists as potentially the first Be ring-containing compound to exhibit aromatic character.

AUTHOR INFORMATION

Corresponding Authors

j.dutton@latrobe.edu.au, david.wilson@latrobe.edu.au

ACKNOWLEDGMENT

We thank The La Trobe Institute for Molecular Science for their generous funding of this project. Generous grants of computing resources from La Trobe University, NCI (project k02) and Intersect are acknowledged. This work was also supported by an ARC Future Fellowship (JLD, FT16010007).

REFERENCES

1. D. Naglav, M. R. Buchner, G. Bendt, F. Kraus and S. Schulz, *Angew. Chem. Int. Ed.*, 2016, **55**, 10562-10576.
2. K. J. Iversen, S. A. Couchman, D. J. D. Wilson and J. L. Dutton, *Coord. Chem. Rev.*, 2015, **297-298**, 40-48.
3. B. L. Scott, T. M. McCleskey, A. Chaudhary, E. Hong-Geller and S. Gnanakaran, *Chem. Commun.*, 2008, 2837-2847.
4. S. A. Couchman, N. Holzmann, G. Frenking, D. J. D. Wilson and J. L. Dutton, *Dalton Trans.*, 2013, **42**, 11375-11384.
5. P. Parameswaran and S. De, *Dalton Trans.*, 2013, **42**, 4650-4656.
6. M. Arrowsmith, H. Braunschweig, M. A. Celik, T. Dellermann, R. D. Dewhurst, W. C. Ewing, K. Hammond, T. Kramer, I. Krummenacher, J. Mies, K. Radacki and J. K. Schuster, *Nat. Chem.*, 2016, **8**, 890-894.
7. B. Kiran, A. K. Phukan and E. D. Jemmis, *Inorg. Chem.*, 2001, **40**, 3615-3618.
8. A. J. V. Marwitz, M. H. Matus, L. N. Zakharov, D. A. Dixon and S. Liu, *Angew. Chem. Int. Ed.*, 2009, **48**, 973-977.
9. P. G. Campbell, A. J. V. Marwitz and S. Liu, *Angew. Chem. Int. Ed.*, 2012, **51**, 6074-6092.
10. Z. X. Giustra and S. Liu, *J. Am. Chem. Soc.*, 2018, **140**, 1184-1194.
11. K. Dehnicke and B. Neumüller, *Zeitschrift für Anorganische und Allgemeine Chemie*, 2008, **634**, 2703-2728.
12. F. Kraus, S. A. Baer, M. R. Buchner and A. J. Karttunen, *Chem. Eur. J.*, 2012, **18**, 2131-2142.
13. R. Puchta, B. Neumüller and K. Dehnicke, *Z. Anorg. Allg. Chem.*, 2011, **637**, 67-74.
14. R. Puchta, B. Neumüller and K. Dehnicke, *Z. Anorg. Allg. Chem.*, 2009, **635**, 1196-1199.
15. B. Neumüller and K. Dehnicke, *Zeitschrift für Anorganische und Allgemeine Chemie*, 2010, **636**, 1516-1521.

16. Y. Sohrin, H. Kokusen, S. Kihara, M. Matsui, Y. Kushi and M. Shiro, *Chem. Lett.*, 1992, 1461.
17. D. Naglav, D. Bläser, C. Wölper and S. Schulz, *Inorganic Chemistry*, 2014, **53**, 1241-1249.
18. D. Naglav, B. Tobey, C. Wölper, D. Bläser, G. Jansen and S. Schulz, *Eur. J. Inorg. Chem.*, 2016, 2424–2431.
19. Y. Qu and Y. Zhang, *Spectrochimica Acta Part A*, 2007, **67**, 350-354.
20. R. Shinde and M. Tayade, *J. Phys. Chem. C.*, 2014, **118**, 17200-17204.
21. L. Ren, Longjiu Cheng, Yan Feng and X. Wang, *J. Chem. Phys.*, 2012, **137**, 014309.
22. M. J. Frisch, G. W. Trucks, H. B. Schlegel, G. E. Scuseria, M. A. Robb, J. R. Cheeseman, G. Scalmani, V. Barone, B. Mennucci, G. A. Petersson, H. Nakatsuji, M. Caricato, X. Li, H. P. Hratchian, A. F. Izmaylov, J. Bloino, G. Zheng, J. L. Sonnenberg, M. Hada, M. Ehara, K. Toyota, R. Fukuda, J. Hasegawa, M. Ishida, T. Nakajima, Y. Honda, O. Kitao, H. Nakai, T. Vreven, J. J. A. Montgomery, J. E. Peralta, F. Ogliaro, M. Bearpark, J. J. Heyd, E. Brothers, K. N. Kudin, V. N. Staroverov, R. Kobayashi, J. Normand, K. Raghavachari, A. Rendell, J. C. Burant, S. S. Iyengar, J. Tomasi, M. Cossi, N. Rega, J. M. Millam, M. Klene, J. E. Knox, J. B. Cross, V. Bakken, C. Adamo, J. Jaramillo, R. Gomperts, R. E. Stratmann, O. Yazyev, A. J. Austin, R. Cammi, C. Pomelli, J. W. Ochterski, R. L. Martin, K. Morokuma, V. G. Zakrzewski, G. A. Voth, P. Salvador, J. J. Dannenberg, S. Dapprich, A. D. Daniels, Ö. Farkas, J. B. Foresman, J. V. Ortiz, J. Cioslowski and D. J. Fox, Gaussian 09, Revision E.1, Gaussian, Inc., Wallingford CT, 2015.
23. Y. Zhao and D. G. Truhlar, *Theor. Chem. Acc.*, 2008, **120**, 215-241.
24. A. Schafer, H. Horn and R. Ahlrichs, *J. Chem. Phys.*, 1992, **97**, 2571-2577.
25. A. Schafer, C. Huber and R. Ahlrichs, *J. Chem. Phys.*, 1994, **100**, 5829-5835.
26. J. Tomasi, B. Mennucci and E. Cances, *J. Mol. Struct. (Theochem)*, 1999, 464.
27. A. V. Marenich, C. J. Cramer and D. G. Truhlar, *J. Phys. Chem. B*, 2009, **113**, 6378-6396.
28. E. D. Glendening, A. E. Reed, J. E. Carpenter and F. Weinhold, NBO 3.1, 2011.
29. A. Rahalkar and A. Stanger, Aroma, See http://chemistry.technion.ac.il/members/amnon-stanger/.
30. E.J. Baerends, T. Ziegler, A.J. Atkins, J. Autschbach, D. Bashford, A. Bérces, F.M. Bickelhaupt, C. Bo, P.M. Boerrigter, L. Cavallo, D.P. Chong, D.V. Chulhai, L. Deng, R.M. Dickson, J.M. Dieterich, D.E. Ellis, M. van Faassen, L. Fan, T.H. Fischer, C. Fonseca Guerra, M. Franchini, A. Ghysels, A. Giammona, S.J.A. van Gisbergen, A.W. Götz, J.A. Groeneveld, O.V. Gritsenko, M. Grüning, S. Gusarov, F.E. Harris, P. van den Hoek, C.R. Jacob, H. Jacobsen, L. Jensen, J.W. Kaminski, G. van Kessel, F. Kootstra, A. Kovalenko, M.V. Krykunov, E. van Lenthe, D.A. McCormack, A. Michalak, M. Mitoraj, S.M. Morton, J. Neugebauer, V.P. Nicu, L. Noodleman, V.P. Osinga, S. Patchkovskii, M. Pavanello, C.A. Peeples, P.H.T. Philipsen, D. Post, C.C. Pye, W. Ravenek, J.I. Rodríguez, P. Ros, R. Rüger, P.R.T. Schipper, H. van Schoot, G. Schreckenbach, J.S. Seldenthuis, M. Seth, J.G. Snijders, M. Solà, M. Swart, D. Swerhone, G. te Velde, P. Vernooijs, L. Versluis, L. Visscher, O. Visser, F. Wang, T.A. Wesolowski, E.M. van Wezenbeek, G. Wiesenekker, S.K. Wolff, T.K. Woo and A. L. Yakovlev, ADF2016, SCM, Theoretical Chemistry, Vrije Universiteit, Amsterdam, The Netherlands, http://www.scm.com.
31. J. G. Snijders, P. Vernooijs and E. J. Baerends, *At. Data Nucl. Data Tables*, 1981, **26**, 483-509.
32. J. Krijn and E. J. Baerends, *Fit Functions in the HFS-Method: Internal Report (in Dutch)*, Vrije Universiteit Amsterdam, The Netherlands, 1984.
33. E. Van Lenthe, E. J. Baerends and J. G. Snijders, *J. Chem. Phys.*, 1993, **99**, 4597-4610.
34. M. Arrowsmith, M. R. Crimmin, M. S. Hill and G. Kociok-Köhn, *Dalton Transactions*, 2013, **42**, 9720-9726.
35. P. Pyykkö and M. Atsumi, *Chem. Eur. J.*, 2009, **15**, 186-197.
36. M. Bayram, Dominik Naglav, Christoph Wölper and S. Schulz, *Organometallics*, 2017, **36**, 467-473.

37. J. Gottfriedsen and S. Blaurock, *Organometallics*, 2006, **25**, 3784-3786.
38. P. v. R. Schleyer, C. Maerker, A. Dransfeld, H. Jiao and N. J. R. v. E. Hommes, *J. Am. Chem. Soc.*, 1996, **118**, 6317.
39. A. Stanger, *J. Org. Chem.*, 2006, **71**, 883-893.
40. R. Carion, V. Liegeois, B. Champagne, D. Bonifazi, S. Pelloni and P. Lazzeretti, *J. Phys. Chem. Lett*, 2010, **1**, 1563-1568.
41. R. Hoffmann, P. v. R. Schleyer and H. F. Schaefer , III, *Angew. Chem. Int. Ed.*, 2008, **47**, 7164-7167.